Sensors and Actuators B 204 (2014) 142–148

Contents lists available at ScienceDirect

Sensors and Actuators B: Chemical

journal homepage: www.elsevier.com/locate/snb

Biopolymer-assisted construction of porous SnO_2 microspheres with enhanced sensing properties

Pan-Pan Jin [a], Xiaoxin Zou [a,*], Li-Jing Zhou [a], Jun Zhao [a], Hui Chen [b], Ye Tian [c], Guo-Dong Li [a,*]

[a] State Key Laboratory of Inorganic Synthesis and Preparative Chemistry, College of Chemistry, Jilin University, Changchun 130012, China
[b] School of Materials Science and Engineering, China University of Mining and Technology, Xuzhou 221000, China
[c] Tianjin Key Laboratory of Applied Catalysis Science and Technology, School of Chemical Engineering, Tianjin University, Tianjin 300072, China

ARTICLE INFO

Article history:
Received 5 April 2014
Received in revised form 5 July 2014
Accepted 17 July 2014
Available online 29 July 2014

Keywords:
SnO_2
Porous structure
Biopolymer
Sodium alginate
Gas sensor

ABSTRACT

Nanoparticle-assembled SnO_2 microspheres with a porous structure are prepared by a biopolymer-assisted synthetic method. The biopolymer used herein is sodium alginate. Besides sodium alginate, an ethylene glycol–water mixed solvent system is also proven to be necessary for the formation of the porous SnO_2 microspheres. The gas-sensing properties of this material are evaluated by a range of gases, and the results show that the gas sensor based on the porous SnO_2 material exhibits the highest sensing response towards ethanol relative to other testing gases. The sensing response of the porous SnO_2 is ~3 and 4 times as high as those of the solid SnO_2 microspheres (which are prepared in the absence of sodium alginate) and the commercially available SnO_2 nanoparticles, respectively. In addition, the porous SnO_2 sensor exhibits a wide response range from 0.5 to 200 ppm for ethanol detection. In the testing range from 0.5 to 200 ppm, the logarithm of the response value shows a good linear dependency on the logarithm of ethanol concentration, indicating that the porous SnO_2 sensor may be used for quantitative detection of ethanol vapor.

1. Introduction

Gas sensors based on semiconducting metal oxides have been extensively used to detect a wide range of gases and organic vapors. The fundamental mechanism of semiconductor sensors primarily depends on the interaction between the chemisorbed oxygen species on the sensor surface and the gas molecules to be detected, which results into observable variation in the electrical resistance of the sensing material. Undoubtedly, the rapidly expanding fields of nanoscience and nanotechnology have accelerated the development of semiconductor sensors [1]. Many materials at nanoscale often show superior sensing properties (e.g., sensitivity, selectivity and/or reliability) to their bulk counterparts, because of their structural advantages such as high surface area and large density of surface reactive sites. Despite many achievements made in the development of various sensing nanomaterials, there are still many challenges ahead. Some of them include (i) large-scale and "green" preparation of nanostructures with a special morphology/composition; (ii) deep understanding of structure-property correlations for a particular sensing nanomaterial; (iii) goal-directed design/engineering of effective sensing nanostructures. This, hence, calls for more research efforts in the nanosensor technology—a burgeoning and fascinating area.

Tin dioxide (SnO_2) – an important n-type wide-band gap semiconductor – is one of promising oxide materials that can be employed in wide gas-sensing applications [2]. In order to improve SnO_2's sensing properties, bulk doping with heteroatoms [3–5] and surface modification with noble metal particles [6–8] or another semiconductors [9,10] were attempted in the past several decades. By comparison, nanostructuring SnO_2 material is a simpler and more cost-effective strategy, and it might also avoid the high cost of noble metals and/or the complexity of multicomponent systems. A considerable amount of research effort, therefore, has been devoted to prepare a variety of SnO_2 nanostructures for sensing applications [11–22]. In particular, hierarchical SnO_2 nanostructures with a porous structure have attracted extensive attention as an important family of sensing materials in recent years [23–30], because of their large surface area, low density and unique morphological feature. For example, with the assistance of cetyltrimethylammonium bromide as the structure-directing agent, Kuang et al. synthesized mesoporous SnO_2 nanospheres and used them as good sensing

* Corresponding authors. Tel.: +86 431 85168318.
E-mail addresses: chemistryzouxx@gmail.com (X. Zou), lgd@jlu.edu.cn, lifind@21cn.com (G.-D. Li).

http://dx.doi.org/10.1016/j.snb.2014.07.085
0925-4005/

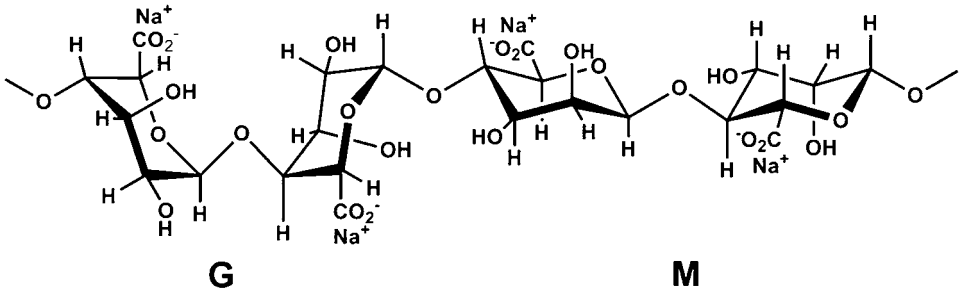

Fig. 1. Structure of sodium alginate containing guluronate (G) and mannuronate (M) units.

materials [23]. Using glucose as the additive, Manjula et al. reported the successful synthesis of porous SnO_2 nanospheres with excellent gas sensing performances for hydrogen detection [24]. In addition, Xie et al. synthesized a porous SnO_2 sensing material in the presence of sodium dodecyl benzenesulfonate (SDBS) and terephthalic acid [26]. Weimar et al. synthesized a SnO_2 porous nanomaterial in a water-in-oil microemulsion system [27], which was established using cetyltrimethylammoniumbromide (CTAB) as a surfactant, hexanol as a cosurfactant and *n*-dodecane as the nonpolar oil phase.

In this paper, we report a facile synthetic route to porous SnO_2 microspheres (p-SnO_2) using biopolymer sodium alginate (NaAlg) as the structure-directing agent for the first time. The as-obtained p-SnO_2 nanomaterial can serve as a highly sensitive material for ethanol detection, thanks to its novel hierarchical structure and porous texture. Notably also, this p-SnO_2 nanomaterial is among the most sensitive SnO_2-based ethanol sensing materials (Table S1, ESI).

Sodium alginate is a naturally available carbohydrate polymer that is composed of mannuronic acid (M-block) and guluronic acid (G-block) units (Fig. 1); and it is also considered as a "green" chemical agent because it is biodegradable and non-toxic. To the best of our knowledge, although sodium alginate has already been used as stabilizer or structure-directing agent for the synthesis of metal and metal oxide nanoparticles [31–38] as well as several metal (hydro)oxide hollow structures [39–43], there were no reports on the biopolymer (sodium alginate)-assisted synthesis of porous SnO_2 nanostructures previously.

2. Experimental

2.1. Reagents and materials

Sodium alginate was purchased from Tianjin Guangfu Fine Chemical Research Institute. Sodium stannate trihydrate ($Na_2SnO_3{\cdot}3H_2O$) was purchased from Tianjin Fuchen Chemical Reagent Factory. Ethanol and ethylene glycol were purchased from Beijing Chemical Works. The reference SnO_2 sample was purchased from Sinopharm Chemical Reagent Co., Ltd. All the above chemicals were used without further purification. Deionized water was used through the experiments.

2.2. Biopolymer-assisted synthesis of porous SnO_2 microspheres

In a typical synthesis of porous SnO_2 material, $Na_2SnO_3{\cdot}3H_2O$ (1.34 g, 5 mmol) was added into ethylene glycol (25 mL) to form solution 1; and sodium alginate (0.25 g) was added into H_2O (25 mL) to form solution 2. Solutions 1 and 2 were mixed under stirring and the resulting mixture was put into a 100 mL Teflon-sealed autoclave, which was then heated at 180 °C for 24 h. After cooled to room temperature, the resulting white precipitate was centrifuged and thoroughly washed with deionized water and ethanol several times, and dried in air at 80 °C. The finally-obtained solid product is the porous SnO_2 material, and this material designated as p-SnO_2. For comparison, the other solid SnO_2 microspheres sample was prepared in the absence of sodium alginate, under otherwise similar synthetic procedures as above. The solid SnO_2 microspheres sample was designated as s-SnO_2.

2.3. General characterization

The powder X-ray diffraction (XRD) patterns were performed with a Rigaku D/Max 2550 X-ray diffractometer using Cu Kα radiation ($\lambda = 1.5418$ Å) operated at 200 mA and 50 kV. The scanning electron microscopic (SEM) images were carried out on a JEOL JSM 6700F electron microscope. The transmission electron microscopy (TEM) and high-resolution TEM (HRTEM) images were obtained on a Philips-FEI Tecnai G2S-Twin. BET surface area and BJH pore diameter were measured by using a Micromeritics ASAP 2020M system.

2.4. Sensor fabrication and testing

The gas sensor was fabricated by pasting viscous slurry of the obtained sample onto a ceramic tube with a diameter of 1 mm and a length of 4 mm, which was positioned with a pair of Au electrodes and four Pt wires on both ends of the tube. A Ni-Cr alloy coil passing through the tube was employed as a heater to control the operating temperature. The schematic structure of the sensor is shown in Fig. 2. For comparison, all of the sensors were fabricated using the same method, and only the difference may be the SnO_2 sensing material. Gas sensing tests were performed on a commercial CGS-8 Gas Sensing Measurement System (Beijing Elite Tech Company Limited).

Gas sensing properties were measured using a static test system which included a test chamber (~1 L in volume). Environmental air with a relative humidity of ~30% was used as both a reference gas and a diluting gas to obtain the desired concentrations of target gases. A typical testing procedure was as follows. After the target gas was injected into the test chamber for about 5 min by a microsyringe, the sensor was put into the test chamber. When the

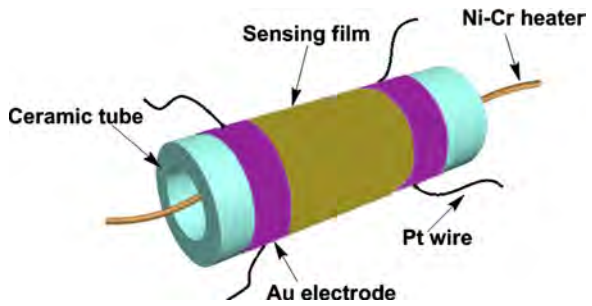

Fig. 2. Schematic diagram showing the structure of a typical gas sensor.

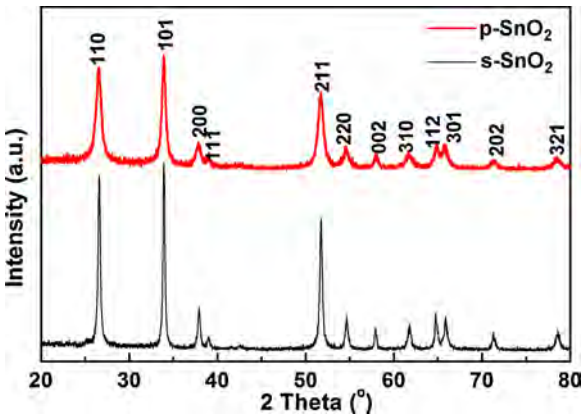

Fig. 3. XRD patterns of p-SnO_2 and s-SnO_2.

response reached a constant value, the sensor was taken out to recover in fresh air. The sensor response is defined as the ratio of R_a to R_g, where R_a and R_g are the electrical resistance of the sensor in atmospheric air and in the testing gas, respectively.

3. Results and discussion

The porous microspheres (p-SnO_2) were hydrothermally synthesized with sodium alginate as the structure-directing agent in an ethylene glycol-water mixed solvent system (v/v = 1:1). Firstly, when sodium alginate was not added in the above mentioned reaction, only nonporous SnO_2 microspheres (i.e., s-SnO_2) were obtained (see below), demonstrating the importance of sodium alginate for the formation of porous structure. Secondly, suitable amount of water in the reaction system was required because sodium alginate can be dissolved in water, but not in ethylene glycol. Thirdly, the presence of ethylene glycol was also very important because when ethylene glycol was not added in the above reaction system, only aggregated SnO_2 nanoparticles (Fig. S1 in ESI) were obtained, indicating that ethylene glycol might be helpful for the self-assembly of SnO_2 nanoparticles. Similar phenomena were also observed in some previous reports on the preparation of hierarchical oxide/hydroxide nanostructures [44,45]. Although the synthesis of the porous SnO_2 microspheres originates from such a multicomponent system, this synthetic approach is facile, controllable and reproducible.

For comparative purpose, s-SnO_2 (which was prepared in the absence of sodium alginate) was also fully characterized, along with p-SnO_2. The XRD patterns of p-SnO_2 and s-SnO_2 are shown in Fig. 3. Both XRD patterns can be well indexed to the tetragonal phase of SnO_2 (JCPDS card No. 41-1445). No XRD peaks of impurities were detected. Moreover, the XRD peaks of p-SnO_2 appear broader than those of s-SnO_2; this indicates that the primary particles in p-SnO_2 are smaller in size than those in s-SnO_2. The crystal sizes of p-SnO_2 and s-SnO_2 were estimated by using the Scherrer formula to be around 9 nm and 21 nm, respectively.

The morphologies of p-SnO_2 and s-SnO_2 were observed by scanning electron microscopy (SEM). The low-magnification SEM image (Fig. S2, ESI) shows that p-SnO_2 consists of spherical particles with a diameter of 200–400 nm. The more detailed structural feature of p-SnO_2 was examined from high-magnification SEM image (Fig. 4A). It is clearly seen that the surface of p-SnO_2 particles is composed of densely packed nanoparticles with several nanometer in size. In addition, some microspheres with a small hollow structure were also seen through some broken particles (see SEM images in Fig. 4B and Fig. S3, ESI). Furthermore, s-SnO_2 also possesses nearly spherical microparticles, but the size of them is much larger than that of p-SnO_2 (Fig. 4C and D). From the above results, it is presumable that the presence of sodium alginate could alter the assembly pattern of SnO_2 nanoparticles.

The transmission electron microscopy (TEM) was used to study the structure of p-SnO_2 and to reveal the structural differences between p-SnO_2 and s-SnO_2. The TEM images of p-SnO_2 (Fig. 5A and Fig. S4, ESI) show a slight lighter region at the center and a continuous darker region around the edges of the microspheres, indicating that the lower particle density at the center of the p-SnO_2 microspheres. In contrast, s-SnO_2 shows a solid structure, demonstrating the importance of sodium alginate in controlling the self-assembly

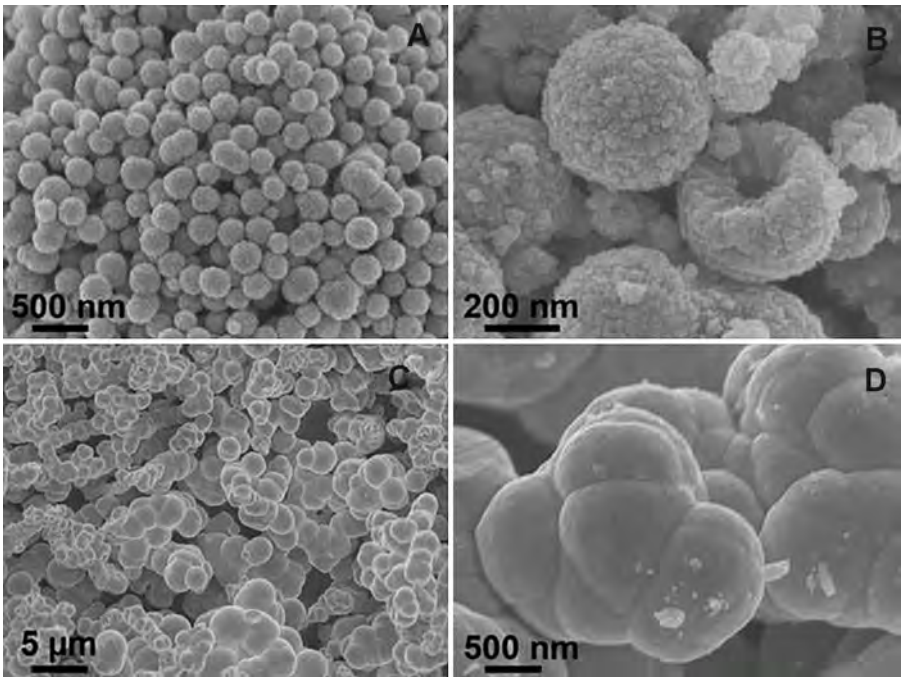

Fig. 4. SEM images of (A and B) p-SnO_2 and (C and D) s-SnO_2.

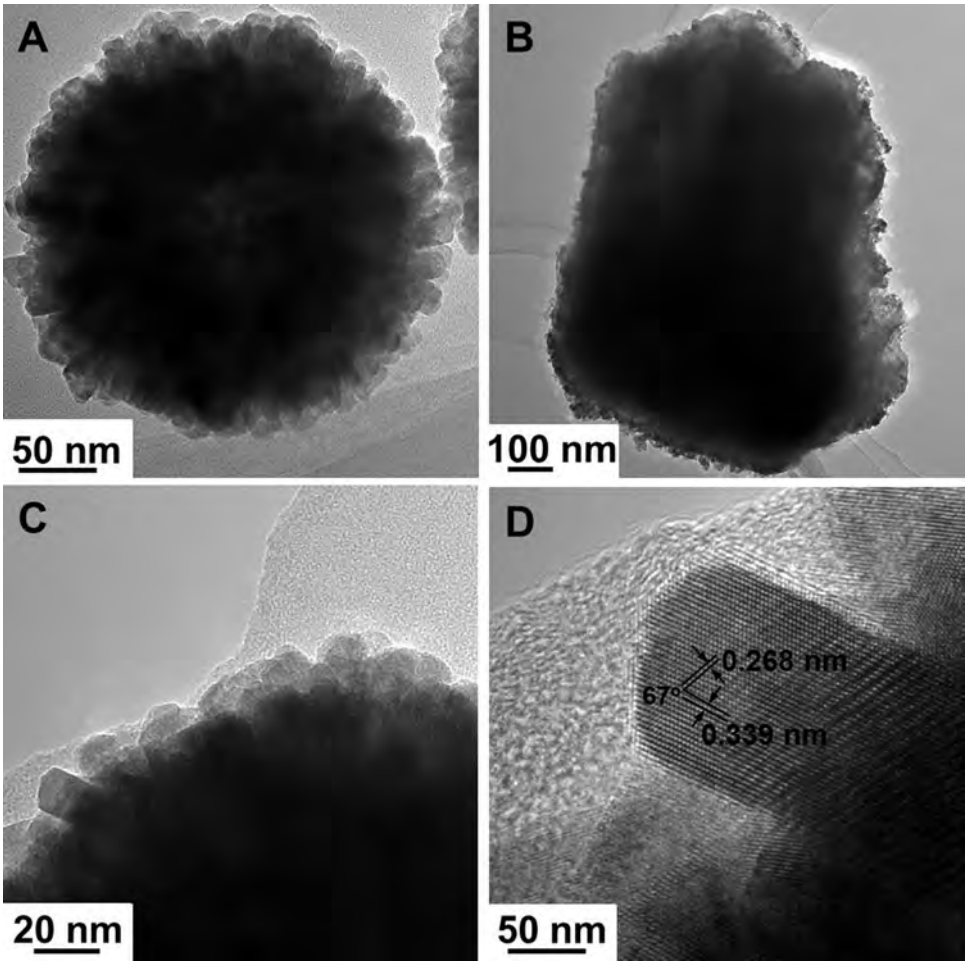

Fig. 5. TEM images of (A) p-SnO_2 and (B) s-SnO_2; and (C and D) TEM and HRTEM images of p-SnO_2.

behavior of SnO_2 nanoparticles. The high-resolution TEM (HRTEM) image of the edge of p-SnO_2 (Fig. 5C) shows the shell to be composed of tightly interconnected SnO_2 nanocrystals of ~10 nm in size. The lattice spacing of the SnO_2 nanocrystals (Fig. 5D) was found to be ~0.268 and 0.339 nm, which is consistent with (1 0 1) and (1 1 0) planes of tetragonal SnO_2.

The N_2 adsorption-desorption isotherms of p-SnO_2 (Fig. 6) exhibit a characteristic type-IV isotherm with an H3 hysteresis loop, indicating the presence of mesoporous/macroporous structure in the material. The corresponding BJH pore-size distribution derived from desorption branch of the isotherm shows a wide pore-size distribution centered at 15 nm, further confirming the existence of mesopores in the material. The corresponding BET surface area of this material is about 29 $m^2\ g^{-1}$, which is large than that (9 $m^2\ g^{-1}$) of s-SnO_2.

Because of its advantageous structural features such as porous structure, it is expected that p-SnO_2 would serve as a good gas sensing material (see the sensor fabrication and testing in experimental section). For comparison, two more gas sensors were fabricated from s-SnO_2 and the commercial SnO_2 nanoparticles with a BET surface area of 6 $m^2\ g^{-1}$ (Com-SnO_2, see the SEM image and the XRD pattern in Fig. S5, ESI). The sensing performance of the SnO_2 materials was evaluated by using ethanol as the testing gas, due to the importance of ethanol sensors in food control applications. The response and recovery times of the sensor are defined as the times taken by the sensor to achieve 90% of the total resistance change. The optimal operating temperature of the SnO_2 sensor was determined by testing 200 ppm ethanol, and the result shows that the optimal operation temperature of the sensor is around 170 °C (Fig. 7). This value is within the scope of temperatures that are usually required to make the semiconductor-based sensors work well, and this operating temperature was applied in all the sensing tests. Note that the target gas was maintained at room temperature (~25 °C) during the whole testing process.

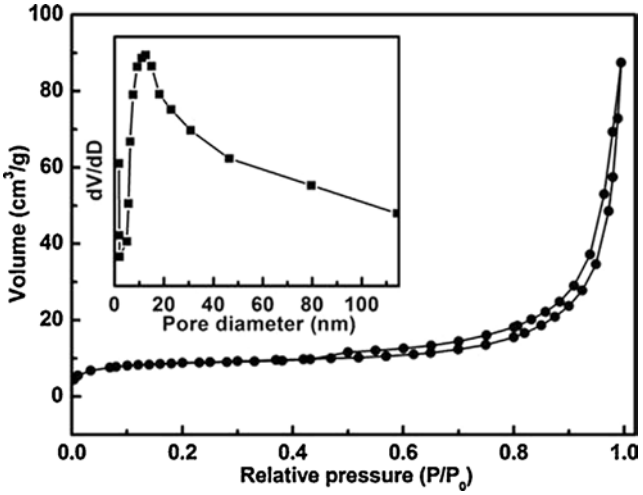

Fig. 6. N_2 adsorption/desorption isotherms for the p-SnO_2 sample with the corresponding pore size distribution shown in the inset.

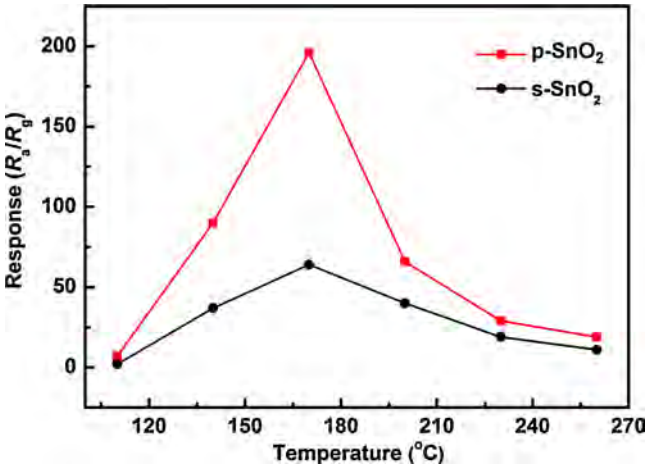

Fig. 7. Response of the sensors based on p-SnO_2 and s-SnO_2 as a function of the operating temperature for the detection of ethanol with a concentration of 200 ppm.

Fig. 8A shows the typical dynamic response-recovery curve of the p-SnO_2 sensor with increasing ethanol concentrations. It is seen that the sensor has a wide response range of 0.5–200 ppm for ethanol detection. The response increases significantly with the increase of ethanol concentration. Moreover, the response is about 1.5 at an ethanol concentration of 0.5 ppm, and thus the detection limit of the p-SnO_2 sensor can be said to be 0.5 ppm. For the concentrations of 0.5, 1, 2, 5, 10, 20, 50, 100, 200 ppm, the responses of p-SnO_2 are about 1.5, 2.5, 4.0, 10, 19, 33, 64, 119 and 197, respectively. In the testing range from 0.5 to 200 ppm, the logarithm of the sensor response shows a good linear dependency on the logarithm of ethanol concentration (Fig. 8B), indicating that the p-SnO_2 sensor may be used as quantitative detection of ethanol vapor. The response times of p-SnO_2 to ethanol are about 25 s, 20 s, 16 s, 7 s, 3 s, 5 s, 2 s, 3 s, and 4 s, for 0.5, 1, 2, 5, 10, 20, 50, 100, 200 ppm, respectively. By comparison, the response times of s-SnO_2 are about 14 s, 6 s, 5 s, 1 s, 2 s, 1 s, 1 s and 1 s for 1, 2, 5, 10, 20, 50, 100, 200 ppm ethanol, respectively. Obviously, the p-SnO_2 exhibits a longer response time for ethanol detection. The stability of the p-SnO_2 sensor was measured by testing 10 ppm ethanol at 170 °C (Fig. S7). Ten almost identical signals were observed in rapid succession in the presence of 10 ppm ethanol, demonstrating the excellent stability of p-SnO_2 sensor. Fig. 8C shows the gas concentration-dependent responses of the sensors based on the p-SnO_2, s-SnO_2 and Com-SnO_2 materials. It is obvious that the p-SnO_2 sensor exhibits response distinctly higher than those of the s-SnO_2 and Com-SnO_2 sensors, demonstrating the importance of a hierarchical structure and porous texture for SnO_2 sensing materials. For example, the sensing response of p-SnO_2 is ~3 and 4 times as high as those of s-SnO_2 and Com-SnO_2, respectively, in the presence of 200 ppm ethanol (Fig. 8C and S6, ESI). Also noteworthy, our p-SnO_2 nanomaterial is among the most sensitive SnO_2-based ethanol sensing materials (see Table S1 in ESI); and only several SnO_2 materials exhibit higher response towards ethanol than p-SnO_2 [12,15,16,46]. The sensing performance of the p-SnO_2 sensor was further investigated by testing a wide range of gases and organic vapors (Fig. 8D). The experimental results show that the p-SnO_2 sensor is more sensitive to ethanol than other gases/vapors including methanol, acetone, formaldehyde, hydrogen, carbon monoxide, benzene, methane and methylamine. From the above sensing results, it is concluded that the p-SnO_2

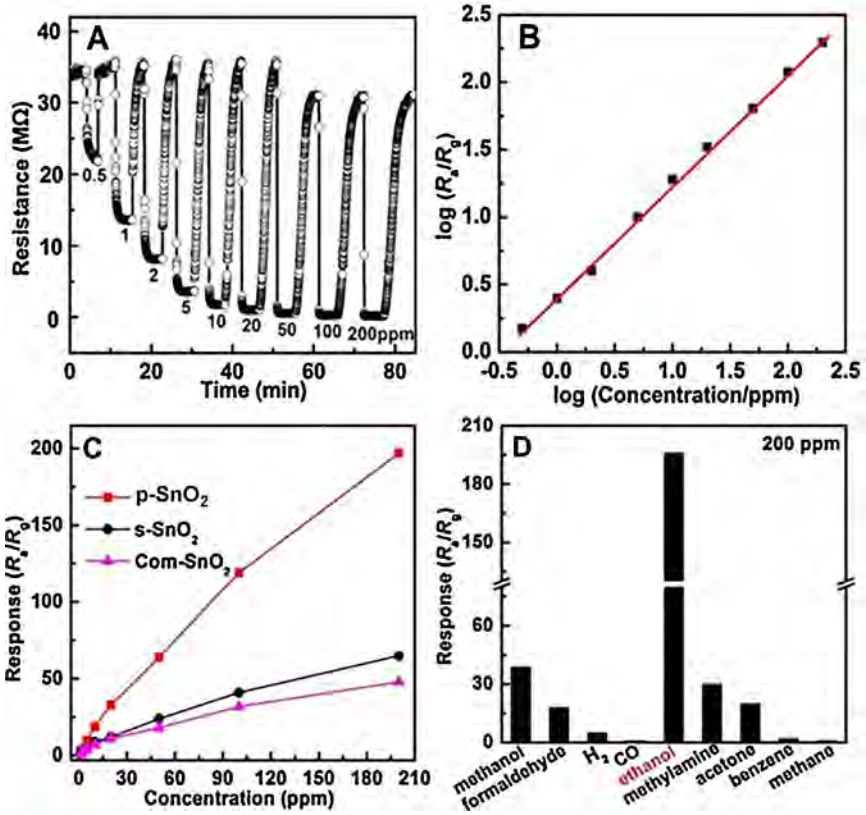

Fig. 8. (A) Dynamic response-recovery curves of the sensor based on p-SnO_2 for ethanol detection; (B) variation of the response (R) of the p-SnO_2 sensor with ethanol concentration (ppm); (C) comparison of the ethanol concentration-dependent responses of the p-SnO_2 sensor, the s-SnO_2 sensor and the Com-SnO_2 sensor; and (D) response comparison of the p-SnO_2 sensor in the presence of different test gases (200 ppm).

nanomaterial is very promising for the fabrication of an ethanol sensor because of its low operating temperature, high response, good selectivity and excellent stability.

4. Conclusions

In summary, we reported the biopolymer-assisted synthesis of porous SnO_2 nanomaterial, which was used as an excellent sensing material for ethanol detection. Both biopolymer sodium alginate and ethylene glycol-water mixed solvent system are necessary for the formation of the porous SnO_2 nanostructure. The significantly improved sensing performance is attributed to its novel hierarchical structure and porous texture. We believe that this study would further promote the exploitation of semiconductor nanomaterial for gas sensors.

Acknowledgement

This work was supported by the National Natural Science Foundation of China (21371070), Natural Science Foundation of Tianjin, China (12JCYBJC14000) and Graduate Innovation Fund of Jilin University (2014052).

Appendix A. Supplementary data

Supplementary data associated with this article can be found, in the online version, at http://dx.doi.org/10.1016/j.snb.2014.07.085.

References

[1] M.E. Franke, T.J. Koplin, U. Simon, Metal and metal oxide nanoparticles in chemiresistors: does the nanoscale matter? Small 2 (2006) 36–50.
[2] A. Tricoli, M. Righettoni, A. Teleki, Semiconductor gas sensors: dry synthesis and application, Angew. Chem. Int. Ed. 49 (2010) 7632–7659.
[3] J.P. Cheng, B.B. Wang, M.G. Zhao, F. Liu, X.B. Zhang, Nickel-doped tin oxide hollow nanofibers prepared by electrospinning for acetone sensing, Sens. Actuators B 190 (2014) 78–85.
[4] L. Liu, C. Guo, S. Li, L. Wang, Q. Dong, W. Li, Improved H_2 sensing properties of Co-doped SnO_2 nanofibers, Sens. Actuators B 150 (2010) 806–810.
[5] P. Song, Q. Wang, Z. Yang, Preparation, characterization and acetone sensing properties of Ce-doped SnO_2 hollow spheres, Sens. Actuators B 173 (2012) 839–846.
[6] H. Zhang, Z. Li, L. Liu, X. Xu, Z. Wang, W. Wang, W. Zheng, B. Dong, C. Wang, Enhancement of hydrogen monitoring properties based on Pd-SnO_2 composite nanofibers, Sens. Actuators B 147 (2010) 111–115.
[7] P. Manjula, S. Arunkumar, S.V. Manorama, Au/SnO_2 an excellent material for room temperature carbon monoxide sensing, Sens. Actuators B 152 (2011) 168–175.
[8] S. Vahdatifar, A.A. Khodadadia, Y. Mortazavia, Effects of nanoadditives on stability of Pt/SnO_2 as a sensing materialfor detection of CO, Sens. Actuators B 191 (2014) 421–430.
[9] Q. Qi, P.P. Wang, J. Zhao, L.L. Feng, L.J. Zhou, R.F. Xuan, Y.P. Liu, G.D. Li, SnO_2 nanoparticle-coated In_2O_3 nanofibers with improved NH_3 sensing properties, Sens. Actuators B 194 (2014) 440–446.
[10] Q. Qi, J. Zhao, R.F. Xuan, P.P. Wang, L.L. Feng, L.J. Zhou, D.J. Wang, G.D. Li, Sensitive ethanol sensors fabricated from p-type $La_{0.7}Sr_{0.3}FeO_3$ nanoparticles and n-type SnO_2 nanofibers, Sens. Actuators B 191 (2014) 659–665.
[11] H. Li, F. Meng, J. Liu, Y. Sun, Z. Jin, L. Kong, Y. Hu, J. Liu, Synthesis and gas sensing properties of hierarchical meso-macroporous SnO_2 for detection of indoor air pollutants, Sens. Actuators B 166–167 (2012) 519–525.
[12] Z. Lin, W. Song, H. Yang, Highly sensitive gas sensor based on coral-like SnO_2 prepared with hydrothermal treatment, Sens. Actuators B 173 (2012) 22–27.
[13] P. Sun, X. Mei, Y. Cai, J. Ma, Y. Sun, X. Liang, F. Liu, G. Lu, Synthesis and gas sensing properties of hierarchical SnO_2 nanostructures, Sens. Actuators B 187 (2013) 301–307.
[14] F. Song, H. Su, J. Han, D. Zhang, Z. Chen, Fabrication and good ethanol sensing of biomorphic SnO_2 with architecture hierarchy of butterfly wings, Nanotechnology 20 (2009) 495502.
[15] W.S. Kim, B.S. Lee, D.H. Kim, H.C. Kim, W.R. Yu, S.H. Hong, SnO_2 nanotubes fabricated using electrospinning and atomic layer deposition and their gas sensing performance, Nanotechnology 21 (2010) 245605.
[16] Y. Jia, L. He, Z. Guo, X. Chen, F. Meng, T. Luo, M. Li, J. Liu, Preparation of porous tin oxide nanotubes using carbon nanotubes as templates and their gas-sensing properties, J. Phys. Chem. C 113 (2009) 9581–9587.
[17] H.C. Chiu, C.S. Yeh, Hydrothermal synthesis of SnO_2 nanoparticles and their gas-sensing of alcohol, J. Phys. Chem. C 111 (2007) 7256–7259.
[18] G. Xi, J. Ye, Ultrathin SnO_2 nanorods: template- and surfactant-free solution phase synthesis, growth mechanism, optical, gas-sensing, and surface adsorption properties, Inorg. Chem. 49 (2010) 2302–2309.
[19] L. Zhang, Y. Yin, Hierarchically mesoporous SnO_2 nanosheets: hydrothermal synthesis and highly ethanol-sensitive properties operated at low temperature, Sens. Actuators B 185 (2013) 594–601.
[20] X. Guo, Y. Kang, L. Wang, X. Liu, J. Zhang, T. Yang, S. Wu, S. Wang, Mesoporous tin dioxide nanopowders based sensors to selectively detect ethanol vapor, Mater. Sci. Eng. C 31 (2011) 1369–1373.
[21] S. Liu, M. Xie, Y. Li, X. Guo, W. Ji, W. Ding, C. Au, Novel sea urchin-like hollow core–shell SnO_2 superstructures: facile synthesis and excellent ethanol sensing performance, Sens. Actuators B 151 (2010) 229–235.
[22] J.P. Ge, J. Wang, H.X. Zhang, X. Wang, Q. Peng, Y.D. Li, High ethanol sensitive SnO_2 microspheres, Sens. Actuators B 113 (2006) 937–943.
[23] Y. Kuang, G. Chen, X. Lei, L. Luo, X. Sun, Mesoporous assembled SnO_2 nanospheres: controlled synthesis, structural analysis and ethanol sensing investigation, Sens. Actuators B 181 (2013) 629–636.
[24] P. Manjula, R. Boppella, S.V. Manorama, A facile and green approach for the controlled synthesis of porous SnO_2 nanospheres: application as an efficient photocatalyst and an excellent gas sensing material, ACS Appl. Mater. Interf. 4 (2012) 6252–6260.
[25] X.M. Yin, C.C. Li, M. Zhang, Q.Y. Hao, S. Liu, Q.H. Li, L.B. Chen, T.H. Wang, SnO_2 monolayer porous hollow spheres as a gas sensor, Nanotechnology 20 (2009) 455503.
[26] Q. Zhao, Y. Gao, X. Bai, C. Wu, Y. Xie, Facile synthesis of SnO_2 hollow nanospheres and applications in gas sensors and electrocatalysts, Eur. J. Inorg. Chem. (2006) 1643–1648.
[27] F. Gyger, M. Hübner, C. Feldmann, N. Barsan, U. Weimar, Nanoscale SnO_2 hollow spheres and their application as a gas-sensing material, Chem. Mater. 22 (2010) 4821–4827.
[28] H. Zhang, Q. He, X. Zhu, D. Pan, X. Deng, Z. Jiao, Surfactant-free solution phase synthesis of monodispersed SnO_2 hierarchical nanostructures and gas sensing properties, Cryst. Eng. Comm. 14 (2012) 3169–3176.
[29] L. Yu, M. Zhang, Y.J. Chen, H.M. Zhang, Q.H. Li, E.D. Zhang, Z. Xu, Assembling SnO_2 nanocubes to nanospheres for high-sensitivity sensors, Solid State Sci. 14 (2012) 522–527.
[30] Z. Li, Q. Zhao, W. Fan, J. Zhan, Porous SnO_2 nanospheres as sensitive gas sensors for volatile organic compounds detection, Nanoscale 3 (2011) 1646–1652.
[31] A. Pal, K. Esumi, T. Pal, Preparation of nanosized gold particles in a biopolymer using UV photoactivation, J. Colloid Interf. Sci. 288 (2005) 396–401.
[32] R. Brayner, M.J. Vaulay, F. Fiévet, T. Coradin, Alginate-mediated growth of Co, Ni, and CoNi nanoparticles: influence of the biopolymer structure, Chem. Mater. 19 (2007) 1190–1198.
[33] E. Kroll, F.M. Winnik, In situ preparation of nanocrystalline (-Fe_2O_3 in iron(II) cross-linked alginate gels, Chem. Mater. 8 (1996) 1594–1596.
[34] M.C. Kimling, R.A. Caruso, Sol–gel synthesis of hierarchically porous TiO_2 beads using calcium alginate beads as sacrificial templates, J. Mater. Chem. 22 (2012) 4073–4082.
[35] Z. Schnepp, S.C. Wimbush, S. Mann, S.R. Hall, Alginate-mediated routes to the selective synthesis of complex metal oxide nanostructures, Cryst. Eng. Comm. 12 (2010) 1410–1415.
[36] S. Dutta, A.K. Patra, S. De, A. Bhaumik, B. Saha, Self-assembled TiO_2 nanospheres by using a biopolymer as a template and its optoelectronic application, ACS Appl. Mater. Interf. 4 (2012) 1560–1564.
[37] S. Gao, Y. Shi, S. Zhang, K. Jiang, S. Yang, Z. Li, E.T. Muromachi, Biopolymer-assisted green synthesis of iron oxide nanoparticles and their magnetic properties, J. Phys. Chem. C 112 (2008) 10398–10401.
[38] Z. Schnepp, S.R. Hall, M.J. Hollamby, S. Mann, A flexible one-pot route to metal/metal oxide nanocomposites, Green Chem. 13 (2011) 272–275.
[39] S. Gao, H. Zhang, X. Wang, R. Deng, D. Sun, G. Zheng, ZnO-based hollow microspheres: biopolymer-assisted assemblies from ZnO nanorods, J, Phys. Chem. B 110 (2006) 15847–15852.
[40] J. Xie, Q. Wu, One-pot synthesis of ZnO/Ag nanospheres with enhanced photocatalytic activity, Mater. Lett. 64 (2010) 389–392.
[41] R. Liu, J. Yin, W. Du, F. Gao, Y. Fan, Q. Lu, Monodisperse CuO hard and hollow nanospheres as visible-light photocatalysts, Eur. J. Inorg. Chem. (2013) 1358–1362.
[42] W. Lu, S. Gao, J. Wang, One-pot synthesis of Ag/ZnO self-assembled 3D hollow microspheres with enhanced photocatalytic performance, J. Phys. Chem. C 112 (2008) 16792–16800.
[43] R. Liu, Y. Jiang, F. Gao, W. Du, Q. Lu, Biopolymer-assisted construction and gas-sensing study of uniform solid and hollow $ZnSn(OH)_6$ spheres, Sens. Actuators B 178 (2013) 119–124.
[44] L.J. Zhou, Y.C. Zou, J. Zhao, P.P. Wang, L.L. Feng, L.W. Sun, D.J. Wang, G.D. Li, Facile synthesis of highly stable and porous Cu_2O/CuO cubes with enhanced gas sensing properties, Sens. Actuators B 188 (2013) 533–539.
[45] L.J. Zhou, C. Li, X. Zou, J. Zhao, P.P. Jin, L.L. Feng, M.H. Fan, G.D. Li, Porous nanoplate-assembled CdO/ZnO composite microstructures: a highly sensitive material for ethanol detection, Sens. Actuators B 197 (2014) 370–375.
[46] L.A. Patil, M.D. Shinde, A.R. Bari, V.V. Deo, Highly sensitive ethanol sensors based on nanocrystalline SnO_2 thin films, Curr. Appl. Phys. 10 (2010) 1249–1254.

Biographies

Pan-Pan Jin is a master student in State Key Laboratory of Inorganic Synthesis & Preparative Chemistry, Jilin University in China. Her research interest is the synthesis of sensing nanomaterials.

Xiaoxin Zou was awarded a Ph.D. in Inorganic Chemistry from Jilin University (China) in 06/2011; and then moved to the University of California, Riverside and Rutgers, The State University of New Jersey as a Postdoctoral Scholar from 07/2011 to 10/2013. He is currently an associate professor in Jilin University. His research interests focus on the design and synthesis of noble metal-free, nanostructured and/or nanoporous materials for water splitting and renewable energy applications.

Li-Jing Zhou received her B.Sc. chemistry degree from Heibei North University, China, in 2009. Presently, she is a Ph.D. student at State Key Laboratory of Inorganic Synthesis & Preparative Chemistry, Jilin University in China.

Jun Zhao received her B.Sc. chemistry degree from Changchun Institute of Technology, China, in 2006. She is a Ph.D. candidate at State Key Laboratory of Inorganic Synthesis & Preparative Chemistry, Jilin University in China.

Hui Chen received his B.E. from Henan Polytechnic University, China, in 2012. He is a graduate student at School of Materials Science and Engineering, China University of Mining and Technology in China.

Ye Tian is a lecturer at Tianjin Key Laboratory of Applied Catalysis Science and Technology, School of Chemical Engineering, Tianjin University in China. He received his B.Sc. (1995), from Tianjin University, and Ph.D. (2007) from Jilin University. His research interests include heterogeneous catalysis and energy process.

Guo-Dong Li is a full professor at State Key Lab of Inorganic Synthesis & Preparative Chemistry, College of Chemistry, Jilin University in China. He received his B.Sc. (1995), M.Sc. (1998) and Ph.D. (2001) from Jilin University. His research interests include chemical sensors, lithium batteries, photocatalysts.